



Causes for the recent increase in sea surface salinity in the north-eastern Gulf of Guinea

Casimir Y. Da-Allada, Gaël Alory, Yves Du Penhoat, Julien Jouanno, Norbert Mahouton Hounkonnou, Élodie Kestenare

► To cite this version:

Casimir Y. Da-Allada, Gaël Alory, Yves Du Penhoat, Julien Jouanno, Norbert Mahouton Hounkonnou, et al.. Causes for the recent increase in sea surface salinity in the north-eastern Gulf of Guinea. *African Journal of Marine Science*, 2014, 36 (2), pp.197-205. 10.2989/1814232X.2014.927398 . hal-01291894

HAL Id: hal-01291894

<https://hal.science/hal-01291894>

Submitted on 22 Mar 2016

HAL is a multi-disciplinary open access archive for the deposit and dissemination of scientific research documents, whether they are published or not. The documents may come from teaching and research institutions in France or abroad, or from public or private research centers.

L'archive ouverte pluridisciplinaire **HAL**, est destinée au dépôt et à la diffusion de documents scientifiques de niveau recherche, publiés ou non, émanant des établissements d'enseignement et de recherche français ou étrangers, des laboratoires publics ou privés.

**Causes for the Recent Increase in Sea Surface Salinity in the north-eastern
Gulf of Guinea**

**Casimir. Y. Da-Allada^{1,2,3}, G. Alory^{2,5}, Y. du Penhoat^{1,3,4}, J. Jouanno^{6,7},
M. N. Hounkonnou² and E. Kestenare³**

¹ International Chair in Mathematical Physics and Applications (ICMPA – UNESCO Chair);
Université d'Abomey-Calavi, 072 BP 50 Cotonou, Bénin

² Université de Toulouse; UPS (OMP); LEGOS; 14 Av, Edouard Belin, F-31400 Toulouse,
France

³ IRD, LEGOS, Toulouse, France

⁴ IRHOB, 08 BP 841 Cotonou, Bénin

⁵ CNAP, LEGOS, Toulouse, France

⁶ IPSL, LOCEAN, Paris, France

⁷ Departamento de Oceanografía Física, CICESE, Ensenada, Baja California, Mexico

Abstract

In situ Sea Surface Salinity (SSS) observations showed an increase $> +0.5$ over the period 2002-2009 in the Gulf of Guinea, off the Niger Delta. Observed changes in the Niger River runoff were not consistent with this increase in SSS, but the increase was reproduced in a regional numerical simulation with climatological river runoff. The simulated mixed-layer salinity budget was used to identify the mechanisms responsible for the increase. When comparing the period 2002-2009 with the period 1993-2001, significant changes in the salt budget were identified. The increase in SSS in the more recent period appeared to be driven by changes in the atmospheric freshwater flux, mainly attributed to a regional decrease in precipitation. Horizontal advection partly compensated for the effect of freshwater flux through changes in zonal currents and zonal SSS gradients.

Keywords: Mixed-layer salt budget, Precipitation, SSS trend

Introduction

Sea Surface Salinity (SSS) is a key indicator of changes in the hydrological cycle at the ocean surface, where most of Earth's freshwater fluxes occur (Yu 2011). Quantifying salinity variability is important, therefore, for understanding global climate change. Curry et al. (2003) showed that SSS increased between the 1960s and the 1990s in the tropical and subtropical North Atlantic, at a rate of 0.02 decade^{-1} . The authors suggested that this SSS increase was caused by increased evaporation associated with global warming of the ocean. Using in-situ observations, Boyer et al. (2005) found that, over the same four decades, the Atlantic Ocean exhibited a large, positive salinity trend (exceeding 0.03 decade^{-1}) in the subtropics and tropics in both the Northern and Southern hemispheres. Grodsky et al. (2006), using a dataset combining the same historical data as the previous studies but with additional data sources that extended to 2004, suggested that the near-surface waters in the tropical Atlantic underwent a major salinification during the period 1960-1985 at a rate of 0.1 decade^{-1} , followed by the reverse trend. Whereas they found that year-to-year changes in salinity were related to precipitation, they attributed decadal salinity changes to wind changes in the deep tropics altering upwelling intensity and, possibly, evaporation rates.

In this study, we use a new in situ SSS gridded dataset for the Atlantic basin (Dallada et al. 2013) to show a recent increase in SSS in the Gulf of Guinea. This increase was also present in a regional simulation of the Tropical Atlantic Ocean from an ocean general circulation model (OGCM) (Jouanno et al 2013). We used the simulated mixed-layer salinity (MLS) budget to identify the mechanisms responsible for this salinification.

We describe (1) the SSS data used in the study and the numerical model employed, and (2) how the model was validated and how it explores changes in the salt budget, freshwater flux and horizontal advection.

71 **Material and methods**

72 **Data and model**

73 **In situ SSS dataset**

74 The observed-SSS product is an updated version of the dataset of Reverdin et al.
75 (2007) described in Da-Allada et al. (2013). The monthly SSS are gridded using an objective
76 mapping (Bretherton et al. 1976) at $1^\circ \times 1^\circ$ spatial resolution, by compiling a variety of data
77 sources, primarily from underway thermosalinographs on research vessels and voluntary
78 observing ships, from the Prediction and Research Moored Array in the Tropical Atlantic
79 (PIRATA) moorings, from surface drifters and from Argo floats. Figure 1 shows the temporal
80 and spatial resolution over the region 15°N - 15°S , 20°W - 15°E for the period 1993-2009. The
81 data distribution increased after 2005 as a result of the deployment of ARGO floats in the
82 region. The overall density of observations presents a marked contrast between areas of poor
83 data coverage (e.g. the south-east region of the Gulf of Guinea) and areas of high density that
84 occur along well-used shipping lines. We chose this SSS product as a reference for model
85 evaluation as it is, to our knowledge, the most complete and up-to-date SSS product available
86 for the Tropical Atlantic basin; salinity has been measured using the practical salinity scale.

87 **Model**

88 The model configuration is based on the Nucleus for European Modelling of the
89 Ocean (NEMO) general ocean circulation modelling system (Madec 2008). It solves the three
90 dimensional primitive equations in spherical coordinates discretised on a C-grid and fixed
91 vertical levels. The model design is a regional configuration of the tropical Atlantic at $\frac{1}{4}^\circ$
92 horizontal resolution. There are 75 levels in the vertical, with 12 in the upper 20 meters and
93 24 in the upper 100 meters. The model is forced at its boundaries (20°S - 20°N and 60°W -
94 15°E) using a radiative open boundary condition provided by outputs from the global
95 interannual experiment ORCA025-MJM95 developed by the DRAKKAR team (Barnier et al.

2006). The vertical turbulent mixing is parameterized using a level-1.5 turbulence closure scheme, with a prognostic equation for turbulence kinetic energy (TKE) and a diagnostic equation for length scale (Blanke and Delecluse 1993).

The atmospheric fluxes of momentum, heat and freshwater were provided by bulk formulae (Large and Yeager 2004) and ERA-Interim reanalysis from the European Centre for Medium-Range Weather Forecasts (ECMWF) (3-hour fields of wind, atmospheric temperature and humidity, and daily fields of long and shortwave radiation and precipitation). This product appears to be the most appropriate in terms of freshwater budget in the Tropical Atlantic (Da-Allada et al. 2013). The short wave radiation forcing is modulated by a theoretical diurnal cycle. A monthly climatology of continental runoffs from Dai and Trenberth (2002) is prescribed near the rivers mouths as a surface freshwater flux. To justify the use of monthly runoff, we tested different simulations (with climatology, yearly and constant river flow) and found that interannual variability of river flow does not have much effect on the interannual SSS in the eastern tropical Atlantic Ocean. It should be noted, however, that uncertainty of the runoff data at interannual time scale is high in this region.

The model was initialized on 1 January 1990, using temperature and salinity outputs from the ORCA025-MJM95 global experiment for the same date, and then integrated over the period 1990-2009. Note that there was no restoring term toward a climatological SSS. Three day averages values of SSS from 1993 to 2009 were used in the present analysis. Jouanno et al. (2013) provide further details on the parameterization and some elements of validation, including comparisons with surface and in-situ observations of temperature in the Gulf of Guinea. Our focus was on the causes of salinification detected in the north-eastern part of the Gulf of Guinea.

Salinity Budget

To investigate the processes of SSS variability at interannual time scales, as described in Ferry and Reverdin (2004), we used a salinity budget in the ocean mixed layer. This approach has been widely used in the tropical Atlantic to investigate the processes controlling the mixed-layer temperature at seasonal time scales (Peter et al. 2006).

Following the study of Vialard et al. (2001), the equation for mixed-layer salinity evolution can be written as follows:

$$\partial_t SSS = \underbrace{-\langle u \partial_x S \rangle}_{UADV} - \underbrace{\langle v \partial_y S \rangle}_{VADV} - \underbrace{\langle w \partial_z S \rangle}_{WADV} + \underbrace{\langle D_l(S) \rangle}_{DIFL} - \underbrace{\frac{(k \partial_z S)_{z=-h}}{h}}_{ZDF} - \underbrace{\frac{1}{h} \frac{\partial h}{\partial t} (SSS - S_{z=-h})}_{ENT} + \underbrace{\frac{(E - P - R)SSS}{h}}_{FWF} \quad (\text{Eq.1})$$

where S is the model salinity, u and v are the eastward and northward components, respectively, of the horizontal velocity, w is the upward vertical velocity, $D_l(S)$ is the lateral diffusion operator, k is the vertical diffusion coefficient, h is the time varying mixed-layer depth, E is evaporation, P is precipitation and R is river runoff.

The terms in Eq.1 represent, from left to right, mixed-layer salinity tendency, horizontal advection (H ADV; H ADV=U ADV+ V ADV), vertical advection (W ADV), horizontal diffusion (DIFL), vertical diffusion (ZDF) at the mixed-layer base, mixed-layer salinity tendency due to variation of the mixed-layer depth, (ENT) and freshwater flux terms (FWF).

The mixed-layer salinity budget was computed online to quantify precisely the contributions of the different processes to the mixed-layer salinity tendency. The mixed layer depth was defined by a density criterion (0.03 kg.m^{-3} , de Boyer Montégut et al. 2004), in order to take into account both temperature and salinity stratifications. As Foltz et al. (2004).

We assumed that mixed-layer salinity is very close to SSS (Foltz et al. 2004). Therefore, simulated mixed-layer salinity was compared to observed SSS to validate the model.

Results

Model validation

The model output of annual mean SSS for the period 1993-2009 was very similar to the observed annual mean (Figure 2a-b). South of 5°S, both the model output and the observations showed high values of SSS in the subtropical gyre, which was probably the result of intense evaporation in this region. Elsewhere, low SSS values are a result of either the Intertropical Convergence Zone (ITCZ) along 5°N, or the runoff from major rivers on the west African coast (e.g. the Niger and Congo rivers, which are located in the vicinity of 5°N and 5°S respectively).

With regard to the SSS seasonal cycle in the Gulf of Guinea, the model correctly reproduced the amplitude and phase of the mixed-layer salinity. In particular, in the northern region of the Gulf of Guinea, the use of an OGCM, which explicitly calculates vertical diffusion, produced model output that more closely matched the observed values than did a simplified mixed-layer model as used by Da-Allada et al. (2013), highlighting the important role of vertical diffusion in the Gulf of Guinea.

Observed and simulated linear trends in SSS are compared in Figure 2 c-d over the period 2002-2009. The model exhibited a large, positive, salinity trend in the eastern tropical Atlantic, with maximum values up to 0.8 occurring in the low salinity regions of the Gulf of Guinea, i.e. off the Niger Delta and along the equator (Figure 2d). Negative salinity trends occurred in small regions, however. The map of the observed data (Figure 2c) shows regions with negative trends (e.g. along the north coast of the Gulf of Guinea, which had negative trends of around -0.2) and with positive trends (that were most prominent off the Niger Delta

(0.8)) and less pronounced at the equator. Both observations and model results showed the greatest increase near the Niger Delta (1°S - 5°N , 6° - 10°E) where the trend was significant (Welch test; $p < 0.05$). Elsewhere trends are lower in amplitude and significance is questionable. Therefore our analysis was focused on this region (see boxes in Figure 2 c-d), referred to hereafter as the focal area.

Interannual SSS anomalies, spatially averaged in the focal area from both the observations and the model output, are shown in Figure 3a. Both time series presented a similar evolution, which showed two periods. The first period was characterized by an absence of notable salinity trend in either the observations or the model output and was termed the 'period of reference' (REF). The second exhibited a fairly large, positive SSS trend of about + 0.5 for the period 2002-2009 (Student's t-test; $p < 0.1$), in both the model output and observations, and was termed the 'period of change' (CHA). The close agreement between the modelled and observed SSS suggests that the model can be used to explore changes in the salt budget responsible for the SSS increase.

Changes in salt budget

Applying the model of Alory and Meyers (2009) to salinity, we compared the mean balance of the salt budget between the periods REF and CHA to investigate possible changes. Figure 3b shows, for both periods and for both the model output and the observations: (1) mean anomalies (and standard deviation) of SSS changes (dS); (2) linear trend of SSS; and (3) the model salt budget terms, computed using a five-year running mean. The use of running means allows the standard deviation to be estimated for each term, which assists with the identification of significant changes in terms of the salt budget.

Change in SSS and the linear trend of SSS in the model were positive for the recent period, CHA, and confirmed an SSS increase in the focal area, which was also detected in the observations data (Figure 3b). In the model output, there was a significant change in SSS

(Welch test; $p < 0.05$) between the two periods, REF and CHA. To identify the primary mechanisms responsible for the SSS change, salinity balance terms were plotted in Figure 3b. Horizontal diffusion and entrainment terms were negligible and were therefore not shown in the figure. Freshwater flux (FWF) and horizontal advection (H ADV) changed significantly (Welch test; $p < 0.05$). Freshwater flux was strongly negative during REF and became strongly positive during CHA, which would explain the increase in SSS. Horizontal advection was slightly positive during REF and became strongly negative during CHA. Hence it contributed to decrease in SSS and tended to compensate for the effect of changes in freshwater flux. Vertical advection (W ADV) and vertical diffusion (ZDF) also changed, but not significantly.

Changes in freshwater flux

Likely causes of the change in freshwater flux were explored. Freshwater flux includes three components: evaporation (E), precipitation (P) and runoff (R). Increasing SSS in the model was not related to a change in river runoff because only climatological run-off was used in Eq.1. Moreover, the interannual variability of the Niger runoff, determined from altimetry according to the method developed by Papa et al (2010), did not exhibit any significant changes during the period 2003-2009, other than a slight increase in 2009 (data not shown).

Mean evaporation from ERA-Interim and from the model (computed through bulk formulae) are presented in Figure 4a-b. Evaporation values were high south of 5°S and low elsewhere in the basin. Changes in evaporation between CHA and REF are shown in Figure 4d. Increase in evaporation was weak in the focal area as well as south of equator. The mean contribution of evaporation to the salt budget (ES/H , where S is salinity and H is mixed-layer depth) was positive (about 18 yr^{-1} ; Figure 4e), with a pattern slightly different than that for evaporation itself due to spatial variation in the mixed-layer depth (data not shown). The

changes in ES/H between the two periods, CHA and REF, were positive (+1) in the focal area (Figure 4f), indicating that changes in evaporation contributed only slightly to the increase in SSS in recent years .

ERA-Interim precipitation was at a maximum at around 5°N due to the ITCZ, and weakened on either side of the ITCZ (Figure 4c). There was a large precipitation decrease between the two periods in our focal area. Precipitation changes over the ocean seem to be linked to precipitation changes over the continent, with a deficit in precipitation around 10°N and an increase south of 5°N, centred on 12°E (Figures 4c and 4g). However, rainfall products are subject to uncertainties. Comparing of ERA-Interim with GPCP (Global Precipitation Climatology Project) version 2.1 (Adler et al., 2003), based on observations, showed some differences, especially on land. However, both products showed a decrease in precipitation in the focal area (Figure 5a) although it was more pronounced in ERA-Interim. The higher-resolution TRMM-3B43 satellite product (Adler et al., 2000) is limited to a shorter period that which precluded a direct comparison between the CHA and REF periods, but there appeared to be negative precipitation trend over the period 1998-2010 in the same focal area (Figure 5b), which is consistent with changes in other products and tends to support our results.

The mean contribution of precipitation to the salt budget was negative ($-PS/H$; -30 yr^{-1}), with a spatial pattern very similar to that for precipitation (Figure 4h). The change in this term between the two periods, CHA and REF, was positive (+3) in the focal area, suggesting that its contribution increased SSS in the salt budget.

Hence it appears that, off the Niger Delta in recent years, precipitation decrease was the dominant term with regard to freshwater-flux, and its contribution to the salt budget led to an increase in SSS.

Changes in horizontal advection

The contribution of the horizontal advection to the salt budget off the Niger River delta changed significantly between the two periods, and tended to decrease SSS in the recent period (Figure 3b), partly compensating the salinification effect of the freshwater fluxes. The mean horizontal advection also contributed to a decrease in SSS in the whole basin (Figure 6a). Changes in horizontal advection had both positive and negative values, depending on regions (Figure 6b), but, on average, were negative in the focal area. This was due mainly to changes in zonal advection because changes in meridional advection contributed only slightly to an increase in SSS (data not shown).

To identify whether changes in zonal currents or zonal SSS gradients were responsible for the changes in H ADV, the mean zonal current, changes in zonal current, mean zonal SSS gradient and changes in zonal SSS gradient were mapped (Figure 6). In the Gulf of Guinea, the mean zonal SSS gradient is mainly negative over the basin, as SSS weakens towards the African coast, and the mean current system consists of the eastward flowing Guinea Current (GC) along the northern coast of the Gulf of Guinea and the westward flowing South Equatorial Current (SEC), with its two branches located on each side of the equator. The model suggests that the strength of both GC and SEC increased in the recent years. In the focal area, comparison between the two periods showed weakening eastward flow and strengthening westward flow, in addition to a mean negative SSS gradient. This contributed to the negative advection term, which partly compensated for the freshwater flux contribution.

Discussion

Interannual variations of SSS during the period 1993-2009 were analysed using a regional numerical simulation and observations. Both model and observations showed a positive, linear trend of SSS since 2002 in the Gulf of Guinea, specifically in a focal area near the mouth of the Niger River delta. The interannual SSS anomalies spatially averaged in this region can be split into two periods: a period of reference (1993-2001), in which SSS was

stable, and a period of change (2002-2009), in which SSS increased significantly. Hosoda et al (2009), when comparing SSS in the world ocean between the period 2003-2007 and the period 1960-1989, also found positive salinity anomalies in the eastern part of the Gulf of Guinea (which were actually the largest in the tropical Atlantic, see their figure 1c), which is consistent with our findings.

We used a simulated mixed-layer salinity budget to identify the changes in the salt budget by comparing the mean balance of the salt budget between the two periods. We have found that SSS increases significantly in the model. In the salt budget, only freshwater flux and horizontal advection changed significantly. Freshwater flux was strongly positive in the recent period, explaining the increase in SSS. Horizontal advection was strongly negative during this period and acted to compensate partially for the effect of freshwater flux. The remaining salt balance terms did not change significantly.

We investigated the causes of these significant changes in freshwater flux and horizontal advection. SSS increase was not related to changes in rivers runoff as we used climatological river runoff in the simulation. Changes in freshwater flux were mainly due to decreasing precipitation in the focal area. These local changes in precipitation may have been related to changes in continental precipitation in neighboring areas. In their investigation of SSS differences between the 1960s and the 1990s at a large spatial scale in the tropical Atlantic, Curry et al. (2003) and Grodsky et al. (2006) also found that atmospheric freshwater fluxes contributed to an increase SSS. In our study, changes in both zonal current and in zonal SSS gradient led to significant changes in horizontal advection. Hence we conclude that this effect dominates the ocean processes and tends to attenuate the effect of freshwater changes.

Grodsky et al. (2006) had previously noted a salinification in the Gulf of Guinea but of a smaller than that found in the current study, probably because they considered a larger region and longer period (1960-1999). Grodsky et al. (2006) also noted a decadal variability

in SSS in addition to an increasing salinity trend in this region, but we cannot conclude if the trend found in our study was part of a decadal signal of SSS or a signature of a longer-time trend. Interestingly, a global analysis also suggested that some of the largest increase in SSS over the period 1950-2008 were found in the Gulf of Guinea (Durack and Wijffels, 2010). Whereas at large scales the hydrological cycle is expected to strengthen in a warming climate and consequently decrease salinity in the wet tropics (Terray et al. 2012), the observed salinification in the Gulf of Guinea suggests that regional changes are driven by more complex processes. The recently available satellite products for SSS (SMOS, Aquarius; Lagerloef 2012; Reul et al. 2012) and the recent increases in ARGO observations in the Gulf of Guinea, will be useful to better understand these processes.

Acknowledgments

The SSS data were extracted from the French SSS observation service, available at <http://www.legos.obs-mip.fr/observations/ssr>. We acknowledge the provision of supercomputing facilities by the CICESE. We acknowledge the PIRATA Project and TAO Project Office at NOAA/PMEL for providing open access to PIRATA data. The regional configuration was set up in cooperation with the DRAKKAR project (<http://www.drakkar-ocean.eu/>). Special thanks are due to Fabien Durand and Frédéric Marin for interesting and fruitful discussions and to Fabrice Papa for computing satellite derived Niger runoff in the recent period. C.Y. D-A would like to thanks the SCAC of the French Embassy in Cotonou, Bénin, and IRD for their support through PhD grants. The authors wish to thank TOTAL S.A. for supporting ICM-PA-UNESCO Chair where this work was completed.

References

- Adler RF, Huffman GJ, Bolvin DT, Curtis S, Nelkin EJ. 2000. Tropical rainfall distributions determined using TRMM combined with other satellite and rain gauge information. *Journal of Applied Meteorology* 39(12): 2007–2023.
- Adler RF, Huffman GJ, Chang A, Ferraro R, Xie P, Janowiak J, Rudolf B, Schneider U, Curtis S, Bolvin D, Gruber A, Susskind J, Arkin P. 2003. The Version 2 Global Precipitation Climatology Project (GPCP) Monthly Precipitation Analysis (1979–Present). *Journal of Hydrometeorology*, 4:1147–1167.
- Alory G, Meyers G. 2009. Warming of the Upper Equatorial Indian Ocean and Changes in the Heat Budget (1960–99). *Journal of Climate*, doi: 10.1175/2008JCLI2330.1.
- Barnier B, Madec G, Penduff T, Molines JM, Tréguier AM, Beckmann A, Biastoch A, Boning C, Dengg J, Gulev S, Le Sommer J, Rémy E, Talandier C, Theetten S, Maltrud M, Mc Lean J. 2006. Impact of partial steps and momentum advection schemes in a global ocean circulation model at eddy permitting resolution. *Ocean Dynamics* 56: 543–567.
- Blanke B, Delecluse P. 1993. Variability of the tropical Atlantic Ocean simulated by a general circulation model with two different mixed-layer physics. *Journal of Physical Oceanography* 23: 1363–1388.
- Boyer TP, Levitus S, Antonov JI, Locarnini RA, Gracia HE. 2005. Linear trends in salinity for the World Ocean, 1955–1998. *Geophysical Research Letter* 32: L01604, doi: 10.1029/2004GL021791.
- Bretherton FP, Davis RE, Fandry CB. 1976. A technique for objective mapping and design of oceanographic experiments. *Deep Sea Research* 23: 559–582.
- Curry R, Dickson R, Yashayaev I. 2003. Ocean evidence of a change in the fresh water balance of the Atlantic over the past four decades. *Nature* 426: 826–829.

341 Da-Allada YC, Alory G, du Penhoat Y, Kestenare E, Durand F, Hounkonnou MN. 2013.
 342 Seasonal mixed-layer salinity balance in the Tropical Atlantic Ocean: Mean state and
 343 seasonal cycle. *Journal of Geophysical Research* 118: doi: 10.1029/2012JC008357.

344 Dai A, Trenberth K. 2002. Estimates of freshwater discharge from continents: latitudinal and
 345 seasonal variations. *Journal of Hydrometeorology*, 3: 660-687.

346 De Boyer Montégut C, Madec G, Fischer AS, Lazar A, Ludicone D. 2004. Mixed layer depth
 347 over the global ocean: An examination of profile data and a profile-based climatology.
 348 *Journal of Geophysical Research-Oceans*, 109: (C12), 52-71.

349 Durack PJ, Wijffels SE. 2010. Fifty-year trends in global ocean salinities and their
 350 relationship to broad-scale warming. *Journal of Climate* 23: 4342-4362, doi:
 351 10.1175/2010JCLI3377.1.

352 Ferry N, Reverdin G. 2004. Sea surface salinity interannual variability in the western tropical
 353 Atlantic: An Ocean general circulation model study. *Journal of Geophysical Research*
 354 109, DOI 10.1029/2003JC002122.

355 Foltz GR, Grodsky SA, Carton JA, McPhaden MJ. 2004. Seasonal salt budget of the
 356 northwestern tropical Atlantic Ocean along 38 °W. *Journal of Geophysical Research*
 357 109: C03052, doi: 10.1029/2003JC002111.

358 Grodsky, SA, Carton JA, Bingham FM. 2006. Low frequency variation of sea surface salinity
 359 in the tropical Atlantic, *Geophysical Research Letter* 33: L14604, doi:
 360 10.1029/2006GL026426.

361 Hosoda S, Suga T, Shikama N, Mizuno K. 2009. Global surface layer salinity change
 362 detected by Argo and its implication for hydrological cycle intensification. *Journal of*
 363 *Oceanography*, 65, 579-586.

364 Jouanno J, Marin F, du Penhoat Y, Sheinbaum J, Molines JM. 2013. Intraseasonal modulation
 365 of the surface cooling in the Gulf of Guinea. *Journal of Physical Oceanography*,
 366 doi:10.1175/JPO-D-12-053.1

367 Large W, Yeager S. 2004. Diurnal to decadal global forcing for ocean sea ice models: The data
 368 sets and flux climatologies. *Rep. NCAR/TN-460+STR, Natl. Cent. For Atmos. Res.*,
 369 Boulder, Colorado.

370 Madec G. 2008. « NEMO ocean engine ». *Note du pole de modélisation, Institut Pierre-Simon*
 371 *Laplace (IPSL), Paris.*

372 Papa F, Durand F, Rossow WB, Rahman A, Bala SK. 2010. Satellite altimeter- derived
 373 monthly discharge of the Ganga - Brahmaputra River and its seasonal to interannual
 374 variations from 1993 to 2008. *Journal of Geophysical Research* 115: C12013, doi:
 375 10.1029/2009JC006075.

376 Peter AC, Le Hénaff M, du Penhoat Y, Menkes CE, Marin F, Vialard J, Caniaux G, Lazar A.
 377 2006. A model study of the seasonal mixed-layer heat budget in the equatorial Atlantic.
 378 *Journal of Geophysical Research* 111: C06014, doi: 10. 1029/2005JC003157.

379 Reverdin G, Kestenare E, Frankignoul C, Delcroix T. 2007. In situ surface salinity in the
 380 tropical and subtropical Atlantic Ocean. Part I. Large scale variability. *Progress in*
 381 *Oceanogry* 73 (3), 311–340. <http://dx.doi.org/10.1016/j.pocean.2006.11.004>.

382 Terray L, Corre L, Cravatte S, Delcroix T, Reverdin G, Ribes A. 2012. Near-Surface Salinity
 383 as Nature's Rain Gauge to Detect Human Influence on the Tropical Water Cycle.
 384 *Journal of Climate* 25: 958-977, doi: 10.1175/JCLI-D-10-05025.1.

385 Vialard J, Menkes C, Boulanger JP, Delecluse P, Guilyardi E (2001) A model study of oceanic
 386 mechanisms affecting equatorial Pacific sea surface temperature during the 1997-1998.
 387 EL Nino. *Journal of Physical Oceanography*, 31 1649-1675.

388 Yu L. 2011. A global relationship between the ocean water cycle and near surface salinity.
389 *Journal of Geophysical Research* 116: C10025, doi: 10.1029/2010JC006937

390 **Figure Captions:**

391 **Figure 1.** Sea surface salinity data distribution indicating the number of $1^\circ \times 1^\circ$ grid points
392 with data in a month as a function of year (top panel). Spatial distribution of the number of
393 months with data in $1^\circ \times 1^\circ$ box for 1993-2009 (bottom panel).

394 **Figure 2.** Annual mean sea surface salinity (SSS) for (a) observations and (b) model ; mean
395 linear trend of SSS build from a 5-year running mean over the period 2002-2009 for (c)
396 observations and (d) model.

397 **Figure 3.** (a) Time series interannual anomalies of SSS: Observations (black), model (red),
398 model trend (dashed blue) and observation trend (dashed purple) for the period REF, and the
399 model trend (blue) and observation trend (purple) for the period CHA. Time series are
400 averaged over the focal area (1°S - 5°N , 6° - 10°E). The mean seasonal cycle is removed and a
401 1-year running mean is applied; (b) SSS changes and SSS trend in model and observation
402 (respectively dS M, trend M, dS O and trend O), and model salt budget terms, averaged over
403 the study box (FWF: freshwater fluxes; H ADV: horizontal advection; W ADV: vertical
404 advection; ZDF: vertical diffusion). A 5- year running mean anomalies for the period of
405 reference (REF) is in blue and the period of change (CHA) is in red.

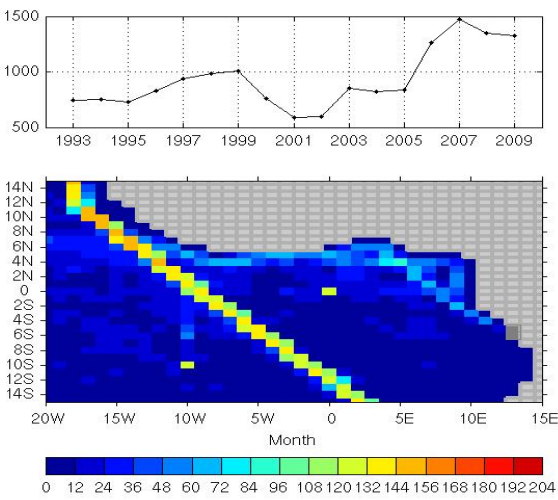
406 **Figure 4.** Annual mean for (a) model evaporation (in mm.day^{-1}), (b) ERA Interim
407 evaporation (in mm.day^{-1}); (c) ERA Interim precipitation (in mm.day^{-1}),; (d) changes in
408 model evaporation (in mm); (e) annual mean contribution to the salt budget for ES/H (E
409 evaporation, S salinity, H mixed layer depth); (f) Changes in ES/H; (g) Changes in ERA-
410 Interim precipitation (in mm); (h) annual mean contribution to the salt budget for $-\text{PS}/\text{H}$ (P
411 precipitation); (i) changes in $-\text{PS}/\text{H}$.

412 Changes are calculated between the period of change (CHA) and the period of reference
413 (REF) build using a 5-year running window. Changes in precipitation and evaporation are

414 calculated using cumulative values for each period. Wind vectors (c) and wind changes
415 vectors (values multiplied by 5) (g) are in m/s.

416 **Figure 5.** a) Changes in GPCP precipitation between CHA and REF periods (in mm) and b)
417 Linear trend over the 1998-2010 period in TRMM-3B43 precipitation (in mm/day/year). The
418 region of study is indicated.

419 **Figure 6.** Horizontal advection annual mean (a) and changes (b); zonal current annual mean
420 (c) and changes (d) in ms^{-1} ; zonal SSS gradient annual mean (e) and changes (f) in m^{-1} .
421 Changes are the difference between the period of change (CHA) and the period of reference
422 (REF) build using a 5-year running window.



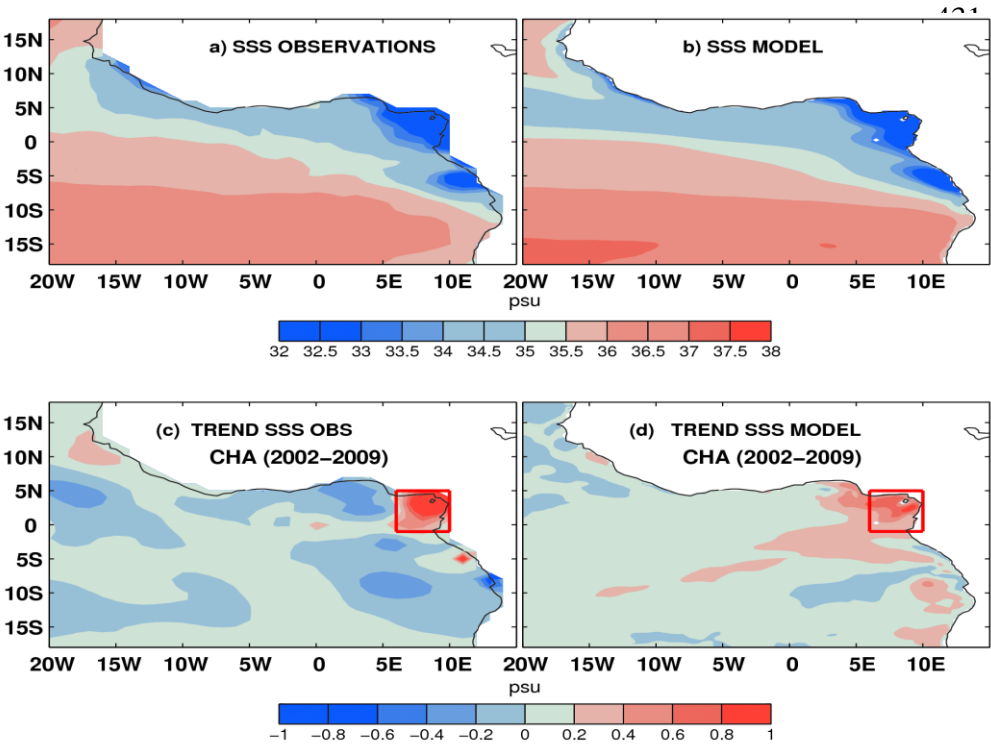
424

425

426 **Figure 1:** Sea surface salinity data distribution indicating the number of $1^\circ \times 1^\circ$ grid points
427 with data in a month as a function of year (top panel). Spatial distribution of the number of
428 months with data in $1^\circ \times 1^\circ$ box for 1993- 2009 (bottom panel).

429

430



442 **Figure 2.** Annual mean sea surface salinity (SSS) for (a) observations and (b) model ; mean
443 linear trend of SSS build from a 5-year running mean over the period 2002-2009 for (c)
444 observations and (d) model.

445

446

447

448

449

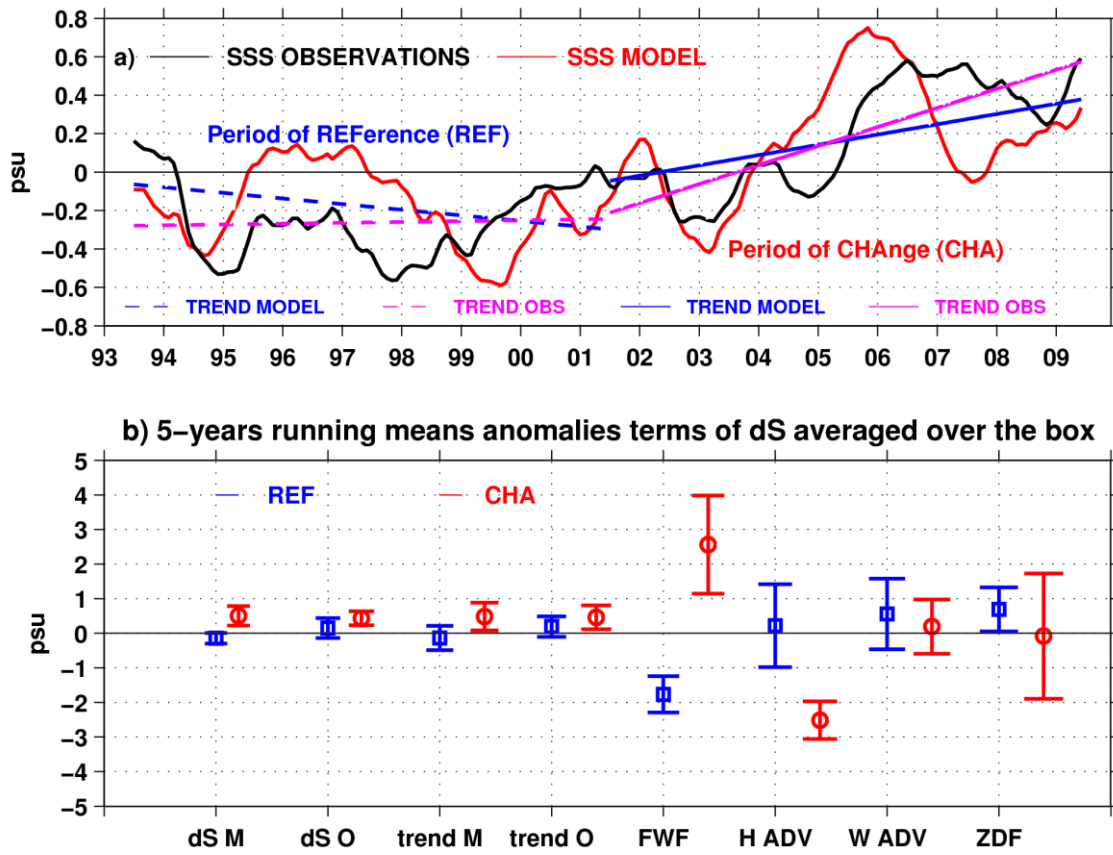
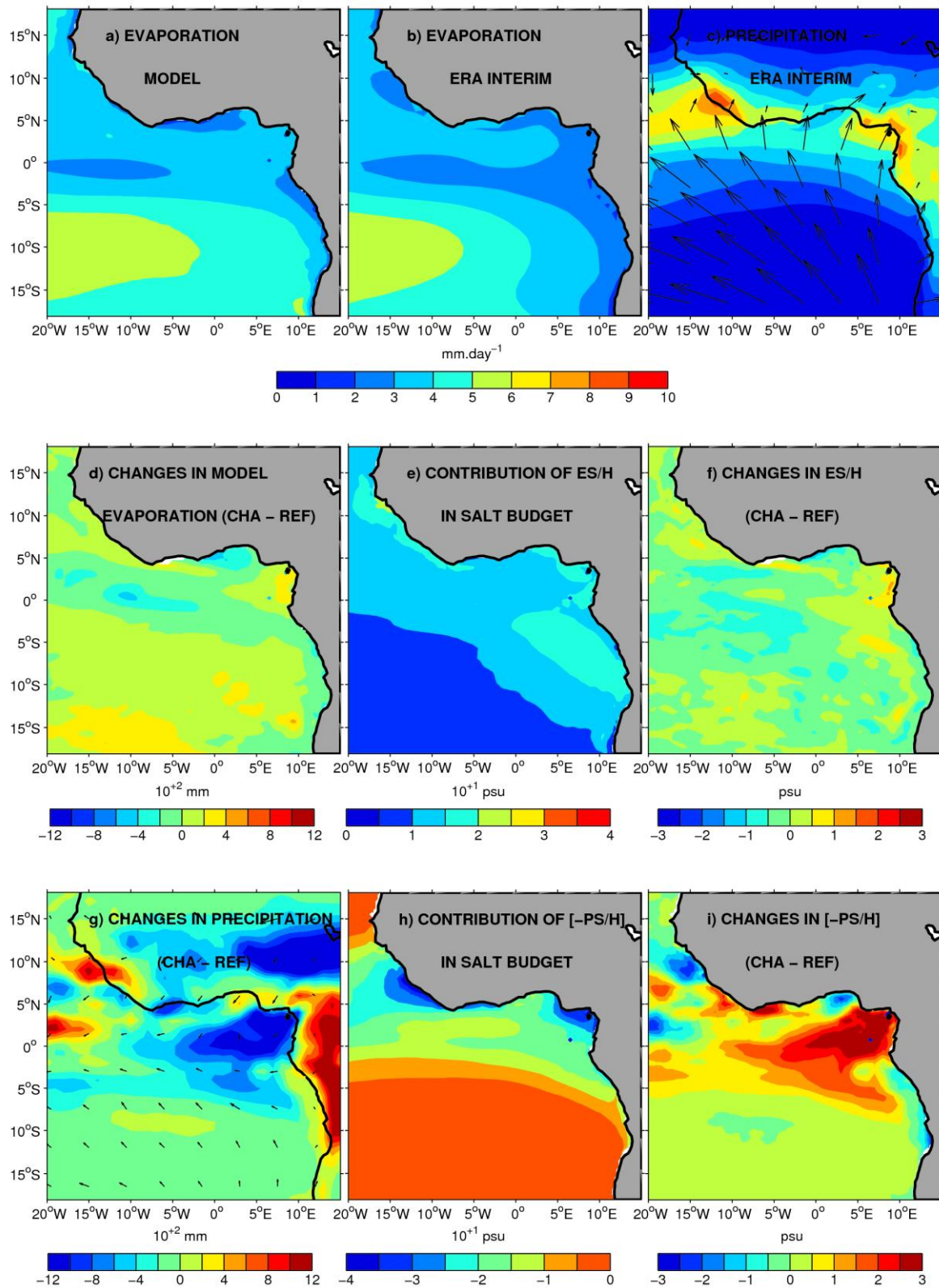


Figure 3. (a) Time series of SSS interannual anomalies: Observations (black), model (red), model trend (dashed blue) and observation trend (dashed purple) for the period REF, and the model trend (blue) and observation trend (purple) for the period CHA. Time series are averaged over the study box (1°S-5°N, 6°-10°E). The mean seasonal cycle is removed and a 1-year running mean is applied; (b) SSS changes and SSS trend in model and observation (respectively dS M, trend M, dS O and trend O), and model salt budget terms, averaged over the study box (FWF: freshwater fluxes; H ADV: horizontal advection; W ADV: vertical advection; ZDF: vertical diffusion). A 5- year running mean anomalies for the period of reference (REF) is in blue and the period of change (CHA) is in red. Units are psu.



463 **Figure 4.** Annual mean for (a) model evaporation (in mm.day⁻¹), (b) ERA Interim
 464 evaporation (in mm.day⁻¹); (c) ERA Interim precipitation ((in mm.day⁻¹); (d) changes in

465 model evaporation (in mm); (e) annual mean contribution to the salt budget for ES/H (E
466 evaporation, S salinity, H mixed layer depth) (in psu); (f) Changes in ES/H; (g) Changes in
467 ERA-Interim precipitation (in mm); (h) annual mean contribution to the salt budget for –
468 PS/H (P precipitation); (i) changes in –PS/H. ES/H and PS/H are the contributions of
469 evaporation and precipitation respectively to the salinity balance.

470 Changes are calculated between the period of change (CHA) and the period of reference
471 (REF) build using a 5-year running window. Changes in precipitation and evaporation are
472 calculated using cumulative values for each period. Wind vectors (c) and wind changes
473 vectors (values multiplied by 5) (g) are in m/s.

474

475

476

477

478

479

480

481

482

483

484

485

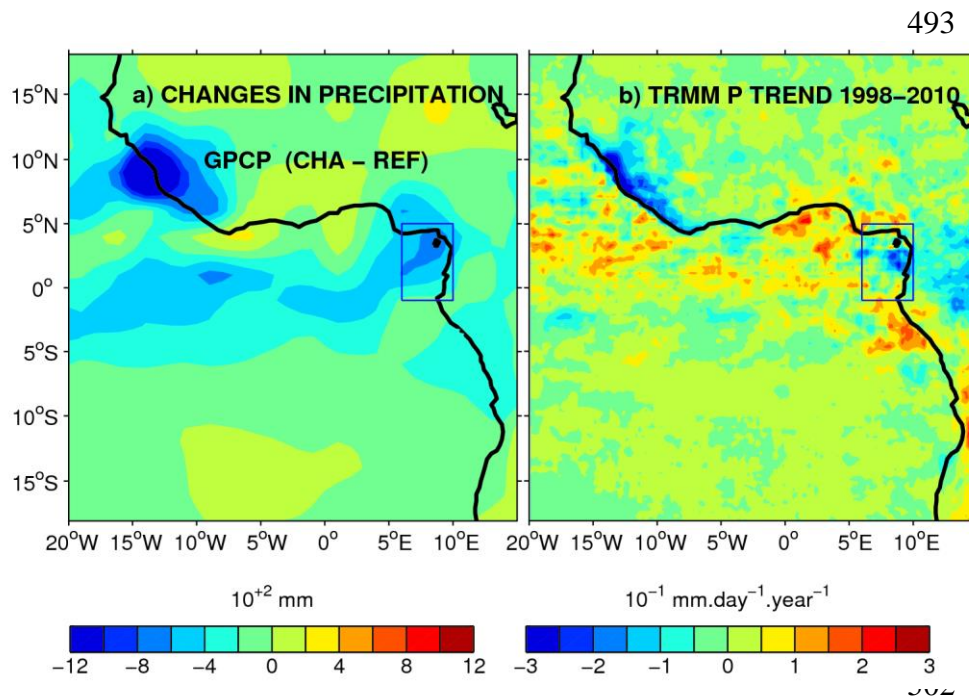
486

487

488

489

490
491
492



503 **Figure 5.** a) Changes in GPCP precipitation between CHA and REF periods (in mm) and b)
504 Linear trend over the 1998-2010 period in TRMM-3B43 precipitation (in mm/day/year). The
505 region of study is indicated.
506
507

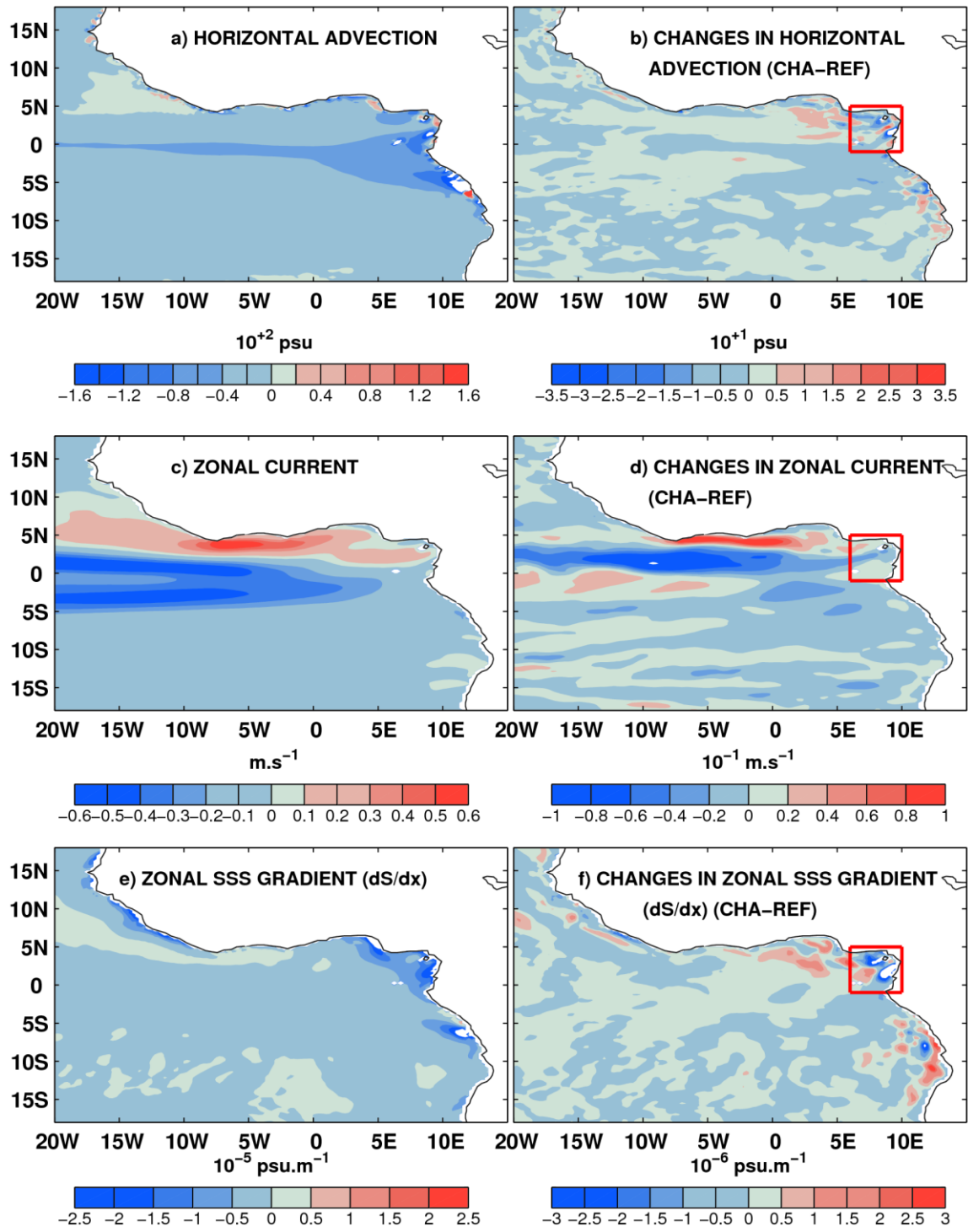


Figure 6. Horizontal advection annual mean (a) and changes (b) in psu; zonal current annual mean (c) and changes (d) in ms^{-1} ; zonal SSS gradient annual mean (e) and changes (f) in

512 psu.m^{-1} . Changes are the difference between the period of change (CHA) and the period of
513 reference (REF) build using a 5-year running window.
514

